Distribution System State Estimation with High Penetration of Demand Response Enabled Loads

Jianzhe Liu, *Member, IEEE*, Ravindra Singh, *Senior Member, IEEE*, and Bikash C. Pal, *Fellow, IEEE*

***Abstract*—Demand-side operations incentivize utility customers to take part in various grid services. A demand response enabled load (DREL) is a flexible grid asset that schedules electricity consumption in response to a time-of-use (TOU) energy price. Consequently, its energy profile differs from that of a conventional load that is insensitive to price. This difference may cause new challenges for distribution system state estimation (DSSE). It is well known that DSSE often needs to use pseudo-measurements based on historic load profiles to increase system observability. However, historic profiles of conventional loads are not representative of DREL behaviors. The inaccuracy impacts DSSE results and other DSSE-dependent operations. In this paper, we propose an online pseudo-measurement generation approach for DSSE with DRELs. We formulate an optimization model to represent DRELs self-adjusting actions. Sampling-based stochastic optimization techniques are proposed to account for uncertainties in DRELs. A set of representative DREL behavior data corresponding to the samples are used to characterize DREL pseudo-measurements. Case studies with modified IEEE 123-bus test system verify the validity of the proposed work.**

I. Introduction

As distributed energy resources (DERs) and advanced load control technologies continue to grow rapidly, recent years have witnessed an emerging integration of loads participating in demand response programs. A demand response enabled load (DREL) adjusts its power consumption according to a time-of-use (TOU) energy price to save revenues by following the signal. As a result, its power output pattern differs from a conventional load that is normally nonresponsive to TOU prices. This poses new challenges for efficiently monitoring and controlling of power distribution assets.

Establishing network visibility is an important first task for a distribution management system (DMS). Usually, a state estimator (SE) accomplishes this task [1]. The SE assists in system supervising and enables many other functions, such as protection, volt-var control, and utility operational planning. The effectiveness of many such DMS functions hinges on the accuracy of the SE [2].

Classic SE is first introduced in the seminal work of Schweppe et al. for transmission systems [3]. It is usually defined as a data-processing algorithm that converts available system information into estimations about magnitude and phase angles of AC bus voltage [4]–[12]. The problem of finding an SE is usually approached through statistical estimation techniques, like weighted least squares (WLS) [3], least absolute value (LAV) [13], and least median square (LMS) methods [14]. The developed SEs have delivered consistent performances, especially when sufficient numbers of high-quality measurements are available.

Recently, distribution system state estimator (DSSE) has been studied [2], [11]. Existing work usually takes into account the special features of a distribution system, including high r/x ratios, radial or weakly-meshed topology, unbalanced and variable loads, among others [4], [15]–[19]. In [4], a branch-current state estimation method is proposed that makes use of the dominantly radial topology in a distribution system to enhance computational efficiency. In [16], non-Gaussian distributed loads are taken into consideration under a probabilistic formulation. In [17], time-varying loads are considered in DSSE when smart meter data of each such load are available. In [19], it is shown that actual load profiles may deviate from the standard load profiles due to the integration of more flexible loads, and probability distributions of individual components are found through statistical study to obtain more realistic power profiles.

One of the most salient challenges for state estimation in a distribution context is that a large portion of a distribution system remains unmonitored; or even if monitored, data are not transmitted for real-time monitoring and control due to communication constraints such as high bandwidth requirements and privacy concerns [20]. Although researchers have proposed various methods for placing limited meters in a distribution system [21], [22], the real measurements alone in a real-world distribution system are usually still inadequate to implement DSSE [2].

Owing to this insufficient data redundancy, pseudo-measurements are used to augment the set of available information. A pseudo-measurement is an estimate of the missing real-time information; it is usually obtained based on historical data or objective predictions [23]. In general, pseudo-measurements are usually generated using one of two main approaches: 1) finding load patterns via analyzing historic data [3]; and 2) using the correlations between the missing data and available real-time measurements [1]. The first approach usually uses empirical probability distributions to find the expected consumption and its variance, based on the assumption that a load follows a consistent pattern. To this end, a variety of probability distribution functions have been developed to model the loads, including Gaussian distribution [24], Gaussian mixture model [25], Weibull distribution [26], log-normal distribution [16], among others. The second approach

Argonne National Laboratory's work was supported by the U.S. Department of Energy, Office of Electricity Delivery and Energy Reliability, under contract DE-AC02-06CH11357.

J. Liu and R. Singh are with the Energy Systems Division, Argonne National Laboratory, Lemont, IL 60439, USA. (email: {jianzhe.liu; ravindra.singh}@anl.gov).

B. Pal is with the Department of Electrical and Electronic Engineering, Imperial College London, London SW7 2AZ, U.K. (e-mail:b.pal@imperial.ac.uk).

commonly needs to recover the correlations between the missing data and the available measurements. The correlation is usually implicit and highly complicated; hence, neural-network-based models have been used to approximate the correlation function [1]. Researchers have investigated neural networks with different structures, such as probabilistic neural network [27], parallel distributed processing network [28], nonlinear auto regressive exogenous model [29], and others. Regardless of the detailed structure, one still needs historic data and real measurements across the system to find model parameters.

Despite the rich literature, there does not seem to be adequate study on DSSE with the integration of DRELs. In addition, existing tools manifest some limitations when considerable DRELs are present. First, most existing historic data are about conventional loads, whereas a DREL normally does not follow the diurnal patterns of a conventional demand. In fact, the consumption behavior of a DREL could be entirely opposite to that of a conventional load. For example, when a DREL participates in peak shaving or valley filling services, it needs to refrain from energy consumption during peak hours of the conventional demands and postpone the usage until valley hours. Second, unlike conventional loads DREL historic data have limited implications for future power outputs. Data about conventional household demands with routine daily living habits can have consistent patterns. However, there is not a consistent pattern for DRELs, because they follow ever-changing energy prices, which means that its historic data are less correlated to future behaviors. Moreover, there are huge variations and uncertainties in the power output of a DREL: 1) the TOU signal has substantial spatial and temporal variability; and 2) a DREL normally installs various DERs and variable loads that have strong dynamics and variability. With these difficulties, directly applying conventional methods will lead to estimates with only limited accuracy.

This paper develops a DSSE framework with a new pseudo-measurement characterization for DRELs. We develop a dynamical model to describe the responsive capability of a DREL, and formulate an optimization problem to approximate a DREL's self-adjusting behavior over available DREL capacity. The problem is structured such that its solution is dependent on a TOU price while satisfying all operational constraints. To account for uncertainties and dynamics of DREL loads, a comprehensive dynamical model is developed to describe the behaviors of a set of loads and resources, including heating, ventilation, and air conditioning (HVAC), energy storage systems (ESSs), plug-in electric vehicles (PEVs), and renewable resources. The model is incorporated in the optimization problem, so that the solution respects operational constraints and user preferences throughout the planning horizon. The parameters of the problem represent the DREL specifics, like the number of PEVs on-site, HVAC initial temperature, and renewable generation. These parameters are considered unknown, representing the uncertainty of DRELs. We apply stochastic optimization techniques to sample the parameters. Solving the optimization problem in the sampled scenarios yields a dataset that is representative of DREL behaviors. Standard load modeling approaches can then be applied to find pseudo-measurements. The contributions of the paper are summarized as follows:

- We have yet to find anyone who has studied the DSSE problem with DRELs; furthermore, we propose a novel pseudo-measurement characterization approach to solve the problem.
- We propose a new DREL modeling approach for DSSE by formulating it as a stochastic optimization problem that yields a set of representative DREL profile data.
- The proposed method is amenable to real-world application. We show how publicly available real-world data can be processed to obtain the required information.
- We show the sensitivity of DSSE accuracy with respect to DREL penetration levels and modeling errors through practical simulation case studies.

The paper is organized as follows: Section II discusses the state estimation problem and a motivating example; Section III shows the main technical results; Section IV uses simulation case studies to demonstrate the value of the proposed work; and Section V concludes the paper.

II. Problem Formulation

A. State Estimation Problem

It is well known that a DSSE solves the following weighted least square (WLS) problem [25]:

$$\min_{x} J = \left(\mathbf{z} - \mathbf{h}(\mathbf{x})\right)^{\top} \mathbf{W} \left(\mathbf{z} - \mathbf{h}(\mathbf{x})\right), \tag{1}$$

where $\mathbf{W}$ is a weight matrix, $\mathbf{z}$ is a measurement vector, $\mathbf{x}$ is the system state to be found, and these two are coupled by, $\mathbf{z} = \mathbf{h}(\mathbf{x}) + \mathbf{e}$, where $\mathbf{e}$ is an error term. The DSSE problem is to find a $\mathbf{x}$ that minimizes J.

WLS (1) is usually a non-convex problem in power system applications due to the nonlinearity in the function $\mathbf{h}(\mathbf{x})$. Different methods exist to solve for a sub-optimum solution to the problem, like convex relaxation and heuristic methods. Below, we show the commonly used Gauss-Newton iteration method. This method generates a sequence of state estimates $\{\hat{\mathbf{x}}\}$, and the limit point of the sequence is used as the estimation result. The k-th element of the sequence is given as follows:

$$\hat{\mathbf{x}}_{k+1} = \hat{\mathbf{x}}_k + \mathbf{G}(\hat{\mathbf{x}}_k)^{-1}\mathbf{H}^{\top}(\hat{\mathbf{x}}_k)\mathbf{W}\left(\mathbf{z} - \mathbf{h}(\hat{\mathbf{x}}_{\mathbf{k}})\right), \tag{2}$$

where $\mathbf{H}(\hat{\mathbf{x}}_k)$ is the Jacobian matrix of function $h(\hat{x})$ evaluated at $\mathbf{x}_k$, and $\mathbf{G}(\hat{\mathbf{x}}_k) = \mathbf{H}^{\top}(\hat{\mathbf{x}}_k)\mathbf{W}\mathbf{H}(\hat{\mathbf{x}}_k)$.

B. Pseudo-Measurement

Notice that in WLS (1), measurement $\mathbf{z}$ needs to be determined before the problem can be solved. If an advanced metering infrastructure exists at every node, the real measurement can be directly used to find $\mathbf{z}$. However, a distribution system is often underdetermined, which means that the dimension of $\mathbf{z}$ composed only by real measurements is usually much smaller than that of $\mathbf{x}$. In such a case, one can use pseudo-measurements to increase the dimension of $\mathbf{z}$ and ensure the observability of the system [11].

Pseudo-measurements are estimates about unmeasured parameters. They are usually generated based on previous knowledge about the unmeasured parameters. For conventional state estimation problems, such parameters are obtained from

abundant historic data. Different methods, such as Gaussian mixture models and artificial neural network methods, have been employed to extract patterns to generate pseudo-measurements [1], [20], [25].

C. Motivating Example

The advancements in load control technology and the development of demand response programs have enabled loads to provide grid services. The power consumption of a demand response enabled load (DREL) is dependent on time-of-use (TOU) rates, which are designed to reflect the changing needs of a power system. As a result, the power profile of a DREL can be highly variable and fundamentally different from that of a conventional load. This is illustrated in Fig. 1, where we show the power profiles of a conventional load and a DREL composed of base loads, energy storage systems, plug-in electric vehicles, among others. The compositions and statistical features of the loads are detailed in Section IV; the dynamics of the loads are described by the models shown in Section III. The figure shows that the DREL profile is significantly different from the conventional profile. Moreover, the DREL power has more variability as the energy price changes rapidly. For example, the DREL creates a steep valley at around hour 11 because the energy price rises. In the following hours, a rebound consumption is observed because price falls.

Conventional methods usually generate pseudo-measurements that share similar patterns. As Fig. 1 demonstrates the high variability of DRELs and their difference against a conventional load, it is required that we develop new pseudo-measurement characterization of DRELs.

III. DREL Pseudo-Measurement

In this section, we develop a DREL pseudo-measurement characterization approach. As shown in Fig. 2, we develop an optimization model to provide representative DREL behavior data to generate pseudo-measurements. We first develop a dynamical model to quantify the flexibility and capability of a DREL to participate in grid services. Then we use an optimization model to mimic the DREL decision-making process subject to quantified DREL capability and various operational constraints. Notice that in the following, the output of the proposed DREL model is a time-series energy consumption profile; and the pseudo-measurements for power injection are approximated by dividing the energy pseudo-measurements by the length of the time step.

Notice that we assume that each DREL is a price-taker that manages its local resources according to energy prices sent from an upstream third-party demand response program. The distribution system operator does not directly participate in either managing the program or local DREL resources. Hence, it is not modeled in this work.

A. Dynamical Model

We develop a discrete-time linear model to characterize a DREL penetrated distribution system node. Using this, we seek to find the collective nodal power profile at the point of interconnection (POI), considering various DREL compositions. The model can be used to represent general

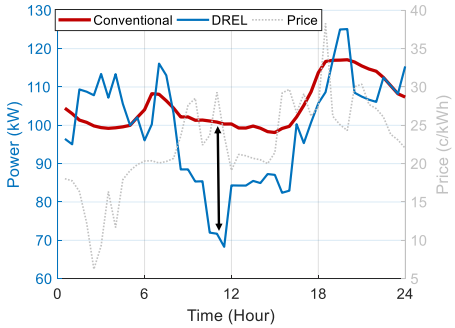

Fig. 1: Conventional and DREL power profiles

DRELs or conventional loads. We exemplify in this subsection how it characterizes multiple representative distributed energy resources (DERs). Specifically, we assume that there are n^{B} energy storage systems (ESSs), n^{H} heating ventilation and air-conditioning (HVAC) systems, n^{V} plug-in electric vehicles (PEVs), and a composite base load with an aggregated photo-voltaic (PV) generation. The ESSs, HVACs, and PEVs are considered to be controllable components. It is worth mentioning that although base loads and PV generation cannot be directly controlled, they can influence the system's responsiveness to TOU rates.

Without loss of generality, we show the model for an arbitrary node indexed by i. We first discuss individual DER models, then show the aggregate model of a DREL node.

1) ESS: We model the charging/discharging behavior of an ESS using a linear discrete time model. Let t be the t-th discrete time interval. Let the state of charge (SOC) of the j-th ESS at the end of t be denoted by $SOC_{i,j}(t) \in [0,1]$, we represent the battery charging/discharging commands as $u^{\mathrm{B}}_{i,j}(t) = [u^{\mathrm{Bc}}_{i,j}(t), u^{\mathrm{Bd}}_{i,j}(t)]^\top \in [0,1]^2$ and the superscript represents that the two variables are of the same domain; the energy output bound is $\bar{E}^{\mathrm{B}}_{i,j}$, the upper bound for SOC change is $\Delta\bar{SOC}_{i,j}$, which is defined as $\bar{E}^{\mathrm{B}}_{i,j}$ divided by the overall battery capacity; and let the charging and discharging efficiency be $\eta^c_{i,j} \in (0,1)$ and $\eta^d_{i,j} \in (0,1)$. Furthermore, let $E^{\mathrm{B}}_{i,j}(t)$ represent the energy consumption of the ESS during time interval t. With the above definition, the battery model is given as follows:

$$\begin{cases} SOC_{i,j}(t+1) = SOC_{i,j}(t) + \Delta\bar{SOC}_{i,j}\left(\eta^c_{i,j} u^{\mathrm{Bc}}_{i,j}(t) - \frac{1}{\eta^d_{i,j}} u^{\mathrm{Bd}}_{i,j}(t)\right) \\ E^{\mathrm{B}}_i(t) = \bar{E}^{\mathrm{B}}_{i,j}\left(u^{\mathrm{Bc}}_{i,j}(t) - u^{\mathrm{Bd}}_{i,j}(t)\right) \end{cases} \tag{3}$$

Notice that the efficiency terms make the model more prone to practical study: charging and discharging commands cannot be operated without any losses in real-world applications. In terms of charging, $(1-\eta^c_{i,j})\bar{E}^{\mathrm{B}}_{i,j} u^{\mathrm{Bc}}_{i,j}$ amount of energy is lost owing to various electrical and thermal losses. The base of the SOC is the rated capacity in the unit of kWh. We only need to use it to determine $\Delta\bar{SOC}_{i,j}$ and the initial SOC, then the evolution of the system dynamics can be fully described by the ESS model. It is also worth mentioning that in the model the charging and discharging commands are continuous variables, opposed to some existing work [30] that treats them

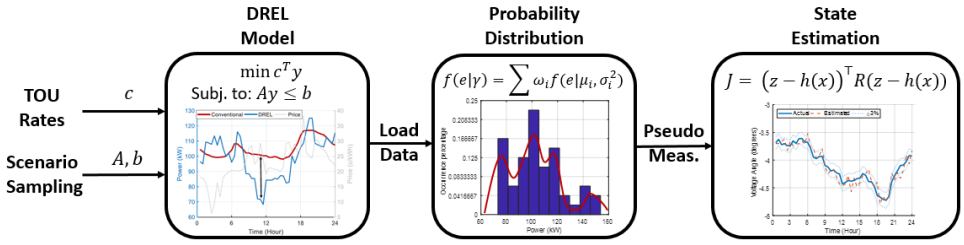

Fig. 2: Proposed DSSE with pseudo-measurement characterization for DRELs

as binary variables. This is because we suppose proper energy management system is installed with the ESS increase its flexibility in energy outputs.

2) HVAC: HVAC represents an important type of flexible loads in demand responses. A typical HVAC system usually involves air handling unit, chillers, and variable air volume boxes [31], so that it has both cooling and heating functions. In this paper, we develop a model that is amenable to direct load control optimization problem formulations, adapted from [31].

We show the model for the j-th HVAC on the node. It is an equivalent thermal circuit model similar to an electrical RLC circuit, where temperature is treated similarly to voltage. The dynamics of indoor temperature are modeled using a capacitor-like heat bank supplied by a heat source modeled as a voltage source. The temperature of the heat source is influenced by both the ambient environment and the HVAC. Let $T^{\mathrm{I}}_{i,j}(t)$ be the indoor temperature, $T^{\mathrm{A}}_{i,j}(t)$ represent the ambient temperature, and $T^{\mathrm{H}}_{i,j}(t)$ represent the temperature adjustment (i.e., cooling and heating) effect of an HVAC. Furthermore, let $u^{\mathrm{H}}_{i,j}(t) = [u^{\mathrm{Hh}}_{i,j}(t), u^{\mathrm{Hc}}_{i,j}(t)]^\top \in [0,1]^2$ represents the HVAC control such that $u^{\mathrm{Hh}}_{i,j}(t) \in [0,1]$ (resp., $u^{\mathrm{Hc}}_{i,j}(t) \in [0,1]$) is heating (resp., cooling) control demand: it works as a slider to determine the heating (resp., cooling) intensity. In addition, $E^{\mathrm{H}}_{i,j}(t)$ represents the energy consumption of the HVAC at time t. The thermal dynamics of an HVAC with respect to power consumption are given as follows:

$$\begin{cases} T^{\mathrm{I}}_{i,j}(t+1) = aT^{\mathrm{I}}_{i,j}(t) + (1-a)\left(T^{\mathrm{A}}_{i,j}(t) + T^{\mathrm{H}}_{i,j}(t)\right) \\ T^{\mathrm{H}}_{i,j}(t) = R\Delta E^{\mathrm{H}}\left(u^{\mathrm{Hh}}_{i,j}(t) - u^{\mathrm{Hc}}_{i,j}(t)\right) \\ E^{\mathrm{H}}_{i,j}(t) = (1-a)\Delta E^{\mathrm{H}}\left(u^{\mathrm{Hh}}_{i,j}(t) + u^{\mathrm{Hc}}_{i,j}(t)\right) \end{cases} \tag{4}$$

where coefficient $a = e^{-\Delta t/CR}$, R and C are the thermal resistance and capacitance, Δt is the duration of one time step, and ΔE^{H} is a constant representing energy transfer rate. This model describes the influences of ambient temperature and an HVAC system on the indoor temperature. As indicated by the model, without any control the indoor temperature eventually converges to the outdoor temperature, $T^{\mathrm{A}}_{i,j}$. Unlike the model developed in [31], we allow $u^{\mathrm{H}}_{i,j}(t)$ to act as a continuous variable and separate the cooling and heating control. Hence, our model can emulate different temperature settings rather than on/off operations.

3) PEV: Charging and discharging behaviors of a PEV can be controlled at a customer site. A PEV becomes controllable when it is being plugged in and is incompletely charged. Meanwhile, it is effectively uncontrollable when it is unplugged or is fully charged. PEV control needs to ensure the required energy and charging deadline are respected. This behavior can be described using a two-dimensional linear model.

We consider the j-th PEV on-site. The state variable of the model is $[RC_{i,j}(t), RW_{i,j}(t)]^\top$, where $RC_{i,j}(t)$ denotes the minimum remaining time to finish the charging task, and $RW_{i,j}(t)$ represents the maximum remaining time to postpone the charging. The control variable represents the command to charge or wait, $u^{\mathrm{V}}_{i,j}(t) = [u^{\mathrm{RC}}_{i,j}(t), u^{\mathrm{RW}}_{i,j}(t)]^\top \in [0,1]^2$, where $u^{\mathrm{RC}}_{i,j}(t)$ is to charge, $u^{\mathrm{RW}}_{i,j}(t)$ is to wait, and $[0,1]^2$ represents that both elements have the same domain of $[0,1]$. Notice that $u^{\mathrm{RC}}_{i,j}(t) + u^{\mathrm{RW}}_{i,j}(t) = 1$, since a vehicle cannot charge and stay idled at the same time. For example, if $u^{\mathrm{RC}}_{i,j}(t) = 1$ the PEV charges for the entire time step. Then although the remaining time necessary for charging is decreased by one, the remaining waiting time is unchanged. With the above-defined variables and parameters, the state dynamics of a PEV is given by:

$$\begin{cases} RC_{i,j}(t+1) = RC_{i,j}(t) - u^{\mathrm{RC}}_{i,j}(t) \\ RW_{i,j}(t+1) = RW_{i,j}(t) - u^{\mathrm{RW}}_{i,j}(t) \\ E^{\mathrm{V}}_{i,j}(t) = \bar{E}^{\mathrm{V}}_{i,j} u^{\mathrm{RC}}_{i,j}(t) \end{cases} \tag{5}$$

where the output variable $E^{\mathrm{V}}_{i,j}$ represents the energy consumption of the PEV at time t, $\bar{E}^{\mathrm{V}}_{i,j}$ is the maximum energy consumption during one time step.

4) Overall Model: The base load and PV generation are considered uncontrollable. We denote their composite energy output as $E^{\mathrm{L}}_i(t)$ and $E^{\mathrm{PV}}_i(t)$ respectively. Notice that models (3), (4), and (5) are all discrete-time linear models sharing a similar structure. For example, we normalize the control input of each DREL component to its potentially diverse bases, hence, each control variable is defined on $[0,1]$. Owing to this trait, their performance can be represented by a more compact one as follows:

$$\begin{cases} x_i(t+1) = A_i x_i(t) + B_{2i} u_i(t) + B_{1i} w_i(t), \\ y_i(t) = D_{2i}^\top u_i(t) + D_{1i}^\top w_i(t). \end{cases} \tag{6}$$

Note that the base load and PV generation are included in system disturbance variable w_i; the output $y_i \in \mathbb{R}$ is a scalar representing the overall energy consumption at the POI of node i. The coefficient matrices can be obtained easily from the individual models. The definition of the states and parameters are available in Appendix A. It is worth mentioning that model (6) can be easily generalized to describe a node when it has none or only a fraction of the above described components.

B. Optimization Model

System (6) models the DREL energy output and its time evolution, hence it characterizes the capability of a DREL to participate in grid services. Next we model how a DREL makes use of the capability to maximize self-profits. The key task lies in simulating DREL responsiveness to TOU prices. The optimal decision making processes can be approximated by an optimization problem.

Without loss of generality, we show the optimization problem for node i at time step zero, and let the optimization horizon be N and let $\mathcal{T} = \{0, \cdots, N-1\}$. The optimization problem is as follows:

$$\min_{u_i(0),\cdots,u_i(N-1)} \sum_{t=0}^{N-1} c(t) y_i(t), \text{ subj. to} \tag{7a}$$

$$x_i(t+1) = A_i x_i(t) + B_{2i} u_i(t) + B_{1i} w_i(t), \quad t \in \mathcal{T}, \tag{7b}$$

$$y_i(t) = D_{2i}^\top u_i(t) + D_{2i}^\top w_i(t), \quad t \in \mathcal{T}, \quad x_i(0) = x_i^0, \tag{7c}$$

$$u_i^{\mathrm{B}}(t) \in [0,1]^{2n^{\mathrm{B}}}, x_i^{\mathrm{B}}(t) \in [\underline{x}_i^{\mathrm{B}}, \bar{x}_i^{\mathrm{B}}], t \in \mathcal{T}, x_i^{\mathrm{B}}(N) = x_i^{\mathrm{BN}}, \tag{7d}$$

$$u_i^{\mathrm{H}}(t) \in [0,1]^{2n^{\mathrm{H}}}, \; x_i^{\mathrm{H}}(t) \in [\underline{x}_i^{\mathrm{H}}, \bar{x}_i^{\mathrm{H}}], \quad t \in \mathcal{T}, \tag{7e}$$

$$u_i^{\mathrm{V}}(t) \in [0,1]^{2n^{\mathrm{V}}}, \quad u_i^{\mathrm{RC}}(t) + u_i^{\mathrm{RW}}(t) = 1, \quad t \in \mathcal{T}, \tag{7f}$$

$$u_i^{\mathrm{RC}}(t) \le RC_i(t), \; u_i^{\mathrm{RC}}(t) \ge 1 - RW_i(t), \quad t \in \mathcal{T}, \tag{7g}$$

$$u_{i,j}^{\mathrm{RC}}(t) = 0,$$
$$\forall t > \min\{N, RC_{i,j}(0) + RW_{i,j}(0)\}, j = 1, \cdots, n^{\mathrm{V}}, \tag{7h}$$

$$y_i(t) \in [\underline{y}_i(t), \bar{y}_i(t)], \quad t \in \mathcal{T}. \tag{7i}$$

Parameter $c(t)$ represents TOU price at time t, hence the cost function (7a) aims at minimizing energy cost. Constraints (7b) and (7c) are the system model and the initial condition, constraint (7i) ensures the POI power output does not exceed operational limitations, and constraints (7d)−(7h) represent the individual operational constraints for DERs and ensure user preferences are respected throughout the optimization horizon.

1) ESS constraint (7d)*:* Constraint (7d) includes the ESS energy output and SOC constraints. They are usually obtained from operational and physical constraints. In addition, it specifies a prescribed level for the end SOC. For example, the SOC level can be regulated to the middle of the operating range to ensure enough capacity to charge and discharge [32].

2) HVAC constraint (7e)*:* Constraint (7e) include the limits for the HVAC energy consumption and the room temperature.

3) PEV constraints (7f)−(7h)*:* Constraint (7f) is the physical energy output bounds and ensures PEVs cannot charge and wait at the same time. Constraints (7g) and (7h) ensure that the desired energy is charged before the deadline.

The parameters of the problem include x_i^0, w_i, and c, in addition to dynamical system parameters. It can be seen that problem (7) is a linear programming problem. If all the system parameters are known, computationally efficient algorithms exist to find the optimal solution. The solution can mimic how a DREL responds to TOU prices.

C. Dataset for Pseudo-Measurement Generation

Notice that the exact values of some of the aforementioned optimization or dynamical model parameters may be unknown in practice. Similar issues exist in stochastic optimization problems where certain variables or parameters are uncertain as well. We apply a scenario-based method to tackle the issue. We assume that a system operator knows the TOU price and has a rough idea of the variation range of the parameters. For example, there are effective data-driven system identification tools to disaggregate nodal power output data into individual system parameters [33].

For simplicity, problem (7) is represented in the following compact form:

$$\min c^\top y_i \quad \text{subj. to: } \bar{A} y_i \le \bar{b}, \tag{8}$$

where $\bar{A}$ and $\bar{b}$ are composite parameters for this problem; with a slight abuse of notation, let $y_i = [y_i(0), \cdots, y_i(N-1)]^\top$ be the composite POI output. Suppose $\bar{A}$ and $\bar{b}$ are unknown but follow given probability distributions. For example, they may follow uniform distributions with known bounds.

Applying Monte Carlo sampling method, we can obtain N^{S} realizations of the unknown parameters. Each realization represents a potential operation scenario with different DREL specifications. Substituting the parameters into (8), the problem becomes well-defined. Therefore, we can obtain the POI output profile $\hat{y}_i^k$ for the select k-th scenario. For each time step t, we can obtain a dataset of DREL profiles, given as $\mathcal{Y}_i(c,t) = \{\hat{y}_i^1(t), \cdots, \hat{y}_i^{N^{\mathrm{S}}}(t)\}$.

Remark 1 (Stopping Criteria). We use a stopping criteria based on coefficient of variation (CV) to determine when to terminate the Monte Carlo simulations. The stopping criteria is set to be 1×10^{-4} in the simulation case study. Recall that for each DREL penetrated bus, we seek to sample the variance of the consumption profile, in order to find the representative distribution of the responses that the DRELs may have with regard to the TOU energy prices. Taking this into account, we terminate the simulation when the change of sample variance is sufficiently small. In Monte Carlo simulations, CV is often used to indicate the dispersion of samplings; in our case study, we suppose that when CV converges (the change of CV is smaller than a threshold) then the change of sample variance is sufficiently small [34]–[36]. In many power engineering research where Monte Carlo simulation methods are applied, like reliability study, researchers often use the convergence of CV as a stopping criteria as well [35]

Remark 2 (Computational Efficiency). The computational efficiency of our work is reasonable. There are two main concerns on this regard: one is whether we need to conduct a large number of the Monte Carlo simulations; and the other is whether optimization problem (8) can be solved efficiently. From our numerical test, the average number of Monte Carlo simulations is around 700 times using the aforementioned stopping criteria when the number of unknown parameters varies from 22 to 52; and using CVX [37] the average computation time for the problem is 0.1 seconds on a laptop with Intel Core i5-1.7GHz 8-core CPU and 16-GB of RAM. Furthermore, as DRELs mostly operate without explicit coordination with the others, each DREL's decision making process can be formulated as an independent problem. This further allows us to reduce the computational burden as parallel computing method can be used to expedite the sampling.

D. Statistical Characteristics of Pseudo-Measurements

Various methods can be applied to find the statistical characteristics of the pseudo-measurements using the dataset. For example, one can utilize Gaussian mixture model (GMM) to describe the statistical characteristics of the data as discussed in our previous work [25]; or machine learning based methods [1], [27] can be used to find pseudo-measurements and integrate them into state estimation problem. Substituting actual measurements and the generated pseudo-measurements into (1), one can find the state estimation for a distribution system penetrated by DRELs. Here, we briefly exemplify how the pseudo-measurements can be generated and integrated into state estimation problem. Suppose we have obtained datasets for the conventional loads or the DRELs, we first use the GMM approximation and mixture reduction method detailed in [18] to approximate its distribution with a GMM. We let each GMM component be a univariate Gaussian distribution, and relevant components can be merged into clusters. Then for time step t, we use the expected value of $y_i(t)$ as the pseudo-measurement. The variance of the pseudo-measurement is obtained by deriving the equivalent Gaussian distribution from the GMM [18], [25]. The pseudo-measurements are used to construct vector $\mathbf{z}$ in (1); and the variances are used to find the weight matrix $\mathbf{W}$ such that $\mathbf{W}$ is a diagonal matrix whose diagonal entries are the reciprocals of the corresponding variances of the measurements [11]. Fig. 3 shows an example of using the aforementioned method to approximate the load distribution with a GMM at Bus 63 of IEEE 123-bus system. The probability density functions of the GMM components are represented in red curves. The overall GMM approximated distribution is the black curve, and it can be seen that the GMM can well represent the original distribution.

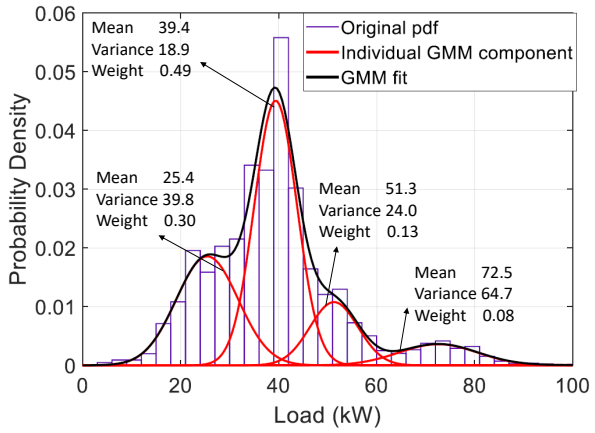

Fig. 3: Example of GMM approximation for load distribution at Bus 63 of the IEEE 123-bus system

IV. Case Studies

In this section, we use simulation case studies based on real-world data to demonstrate the validity of the proposed approach. The case studies are based on a three phase unbalanced IEEE 123-bus system as shown in Fig. 4. The IEEE 123-bus system has 197 power lines and 91 loads [38]. It has been used ubiquitously as a test system to examine SEs. We show that the proposed methods are amenable to real-world application as the required system information can be easily obtained.

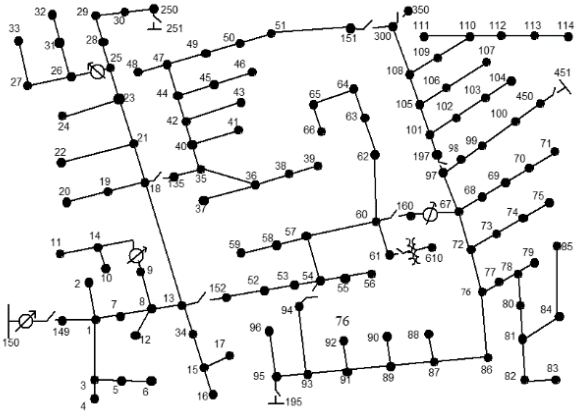

Fig. 4: IEEE 123-bus system [38]

A. Setup

Suppose there are 18 current sensors implemented in the system and one voltage sensor at the substation to provide real measurement data. We use pseudo-measurements to represent all the loads for DSSE purpose. Furthermore, the DRELs reside in 10 nodes, the DREL penetrated nodes correpond to 15% of the overall load demand. Each DREL penetrated node is illustrated in Fig. 5. The available real measurements and sites of the DRELs are summarized in Table I, where I_{i-j} represents the complex current flows in power line connecting bus i and j, and Bus $i.j$ stands for phase j of bus i. In this study, the current measurements are the real and imaginary parts of the three-phase currents, and the voltage measurements are the three-phase voltage magnitude and phase angles at the outgoing terminal of the substation transformer [39]. The real measurements are assumed to have a standard deviation corresponding to 3% error, which is a commonly used set-up for real measurement accuracy in the literature [25] and is aligned with the accuracy of commercial meters like the current transformers designed in accordance with standard IEC 60044-1 accuracy class 1.0 [40], [41]. Notice that higher accuracy in measurement data can improve the estimation results, but the applicability of the proposed work does not depend on the accuracy level of measurement data. In addition, except for switches connecting bus 18-135 and 54-94, all the other switches are assumed to be closed.

TABLE I: Summary of Real Measurements and DREL Sites

Real Measurements	DREL Sites
V_{150}	Bus 1.1, Bus 11.1
$I_{1-2}, I_{3-4}, I_{7-8}, I_{5-6}, I_{8-13}$	Bus 22.2, Bus 30.3
$I_{15-16}, I_{18-21}, I_{23-25}, I_{26-27}, I_{26-31}$	Bus 37.1, Bus 48.3
$I_{36-38}, I_{40-41}, I_{44-45}, I_{51-151}, I_{65-66}$	Bus 49.2, Bus 76.1
$I_{74-75}, I_{78-80}, I_{91-93}$	Bus 88.1, Bus 98.1

To better investigate DREL time-varying characteristics, we need to obtain their time-series power profiles. The manuals of IEEE test systems usually only contain a snapshot of the

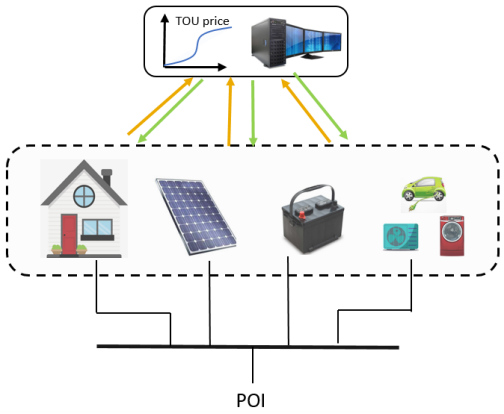

Fig. 5: DRELs at one node

system loading condition. We use real-world data to obtain the time-series power profiles.

First, PEV charging behaviors are obtained from historical data about PEVs or regular vehicles. We exemplify it using National Household Travel Survey (NHTS) 2017 data. NHTS 2017 data records the daily travel history of anonymous users. Although it does not specify whether the users are driving PEVs, useful information can be extracted to represent PEV behaviors. For example, it records the time when users make their last trip home and the moment they leave for work. These data are used to find the probability distributions of the start and end time of a charging event. Second, for weather-related information like temperature and PV generation data, one can resort to weather report or measurement tools that are easily available. For example, the solar radiation information is commonly available from measurement devices of a PV panel, and it can be used to estimate the PV generation in a region. In this case study, we use PV power generation profiles from Solar Radiation Research Laboratory of National Renewable Energy Laboratory [42].

We use real utility customer data to generate base load power consumption profiles. Seven classes of distribution loads are considered in this paper, namely residential loads: single residential loads with and without heating loads, multi-residential loads with and without heating loads; and non-residential loads: commercial loads, non-residential loads with daily consumption smaller than 100 kWh, and non-residential loads with daily consumption between 100−400 kWh. The typical power profiles of these types are shown in Fig. 6. They are representative utility loads. For example, the load with 100−400 kWh daily consumption may represent some office loads, because the weekday peak happens in the middle of the day, while the weekend profile is much flatter. We assume each node in the system to have a time-varying consumption profile. Despite the different profiles, the power averaged over a day is set to be the snapshot power provided by the IEEE 123-bus manual. For example, in the manual the real power consumption at phase A of bus 76 is 105 kW. Fig. 7 shows four load profiles, each of which has 105 kW as the average power but with different compositions. The specified load compositions are shown in Table II. Using the utility data along with other data-processing methods discussed above, the parameters in system (6) can be obtained; hence the behaviors of DRELs can be emulated in the simulation. The TOU energy price is real-time energy price signals obtained from PJM [43], so all the parameters of optimization problem (7a) can be found as well to apply the proposed work. Samples of the DREL and conventional load profiles are shown in Fig. 8. In the figures, the red curves represent the conventional load profiles while the blue curves represent the DREL profiles. It can be seen that the DRELs have more variability and have large deviations from the convention profile. This shows that the DRELs vary the outputs in response to the energy prices in order to reduce costs, and its consumption pattern is different from a conventional load. The sampled data are used to generate pseudo-measurements to assist in our state estimations. Furthermore, the unknown parameters include the initial SOC of the ESSs, PEV charging starting and ending time, PEV required energy, HVAC initial temperature, base load and PV generation. We suppose that the DRELs are incentivised to provide the values for the other parameters.

In this paper, we mainly consider the DRELs with real power responses and let the power factors at each node remain constant that are equal to those provided in the IEEE 123-bus manuals [38]. With this assumption, when the sampling of the real power profiles are obtained, we can directly find the reactive power profiles as well; in addition, the distributions of the reactive power is similar to that of the real power. For example, suppose the real power data follow a Gaussian distribution with mean 60 and variance 16, and let the ratio of real power over reactive power be two. Then the generated reactive power data follow a Gaussian distribution with mean 30 and variance 4. It is worth mentioning that the general idea of the proposed pseudo-measurement characterization method can be applied to the application of DSSE with DRELs responding to other time-varying operational signals, like reactive power demand response signals or voltage regulation [30] as well.

B. Case Study 1

We first test the accuracy of the proposed work. For the simulation case study, we separate available data into two groups: one is known to the state estimator and is considered as historical data; the other is unknown and used for conducting the testing. The former group of data is used to generate the pseudo-measurement and the latter is treated as actual data in the testing. Utilizing the proposed work, the estimated values of voltage magnitude and angles are obtained, as shown in Fig. 9. The actual states are plotted in blue curves while the estimated ones are plotted in orange dotted curves. It can be observed that both the voltage magnitude and angles are estimated accurately using the proposed work. In addition, for the entire day, the state estimation accuracy level remain similar. From 1000 statistical trials, the average root mean square error (RMSE) is 2.08%. To exemplify the estimation accuracy, we show the absolute errors of the voltage magnitude and phase angles in Fig. 10 and Fig. 11 for one trial. Notice that the bus number is modified following the set-up of [39] as

some bus numbers in the original system are not consecutive. Each grey line represents the absolute error profile in a time step, and we show 48 profiles in each subfigure which correspond to the estimation error of a whole day. One can observe that the proposed method can provide a reasonable estimation of the voltage magnitude and phase angles of the entire system, because most magnitude absolute errors are below 0.05 p.u. and angle absolute errors are below 5 degrees, regardless whether the estimated states are near or far away from real measurements. Another observation is that the estimations associated with the buses that are nearer to the substation have relatively higher accuracy owing to the impact of the real measurements at the substation.

In the online exercise of the proposed work, we iterate the following Monte Carlo trial: we sample a realization of all the unknown parameters; with the sampled parameters plugged in the optimization problem, we solve the problem to find the optimal solution, which is an estimated energy output profile; we include the estimated profile into a dataset of the previously obtained estimations and calculate the CV; if CV reaches the prescribed threshold 1×10^{-4}, the sampling procedure is stopped, and we find the GMM; otherwise, we iterate the aforementioned process. In average, the whole procedure takes about 73 seconds of CPU time on a laptop with Intel Core i5-1.7GHz 8-core CPU, 16-GB of RAM, and open-source optimization solver CVX.

C. Case Study 2

In this case study, we use historical data of DRELs to generate DREL pseudo-measurements to compare with the proposed method. The simulation results show that the proposed method still has better estimation accuracy (root mean squared error: 2.08% vs 5.78%) because it can better model the responsiveness of DRELs to variations in energy prices.

To obtain meaningful historical data to represent DREL's previous responsiveness to energy prices, we extract one year (from 09/02/18 to 09/01/19) of the PJM locational marginal pricing (LMP) energy prices [44] at the pricing node *Easton*; and use the energy prices to guide the operation of DRELs for a year. The resulting DREL energy outputs are considered as the historic DREL data. To generate pseudo-measurements, we apply existing work [24] to fit the historical data with Gaussian distributions. Then we use the expected output as the pseudo-measurements and use the variance to tune the weight matrix. Similar to the proposed work, we can thus solve a weighted least square problem to find the estimated states.

We compare the state estimation results of the new benchmark with the proposed method for the day of 09/02/19, which is the next day of the one-year period used to generate historic data. The energy price of the PJM pricing node Easton of that day is used to generate the actual DREL profile as well. It can be seen in Fig. 12 that the expected energy outputs are not a good approximation of the particular consumption profile on 09/02/19, because the energy price on 09/02/20 is different from the average energy price of the previous year as shown in Fig. 13. The RMSE of the benchmark is 5.78% as opposed to 2.08% of our work.

One reason for the difference is that our method explicitly take the variations of the current energy prices into consideration when estimating the DREL behaviors. Consequently, we

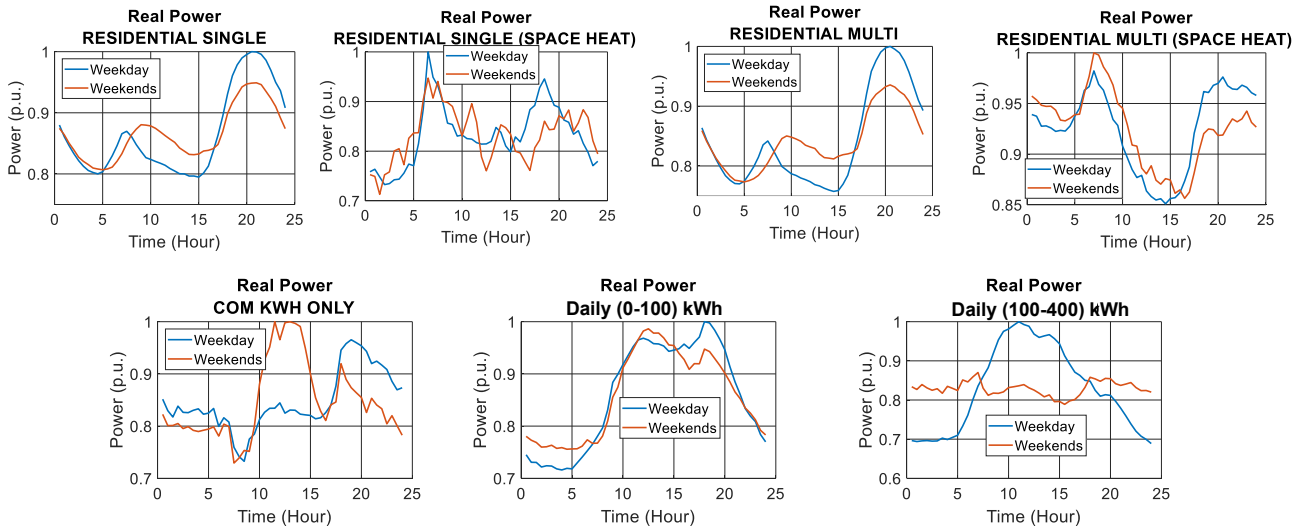

Fig. 6: Example power profiles of seven types of utility customers

TABLE II: Different compositions of loads at phase A of bus 76

	Single	Multi	Single w/ Heat	Multi w/ Heat	kWh Only	Small (0−100 kWh)	Med (100−400 kWh)
Composition 1	40%	30%	10%	0	10%	10%	0
Composition 2	10%	0	30%	0	0	0	60%
Composition 3	10%	10%	30%	30%	20%	0	0
Composition 4	14%	14%	15%	14%	14%	14%	15%

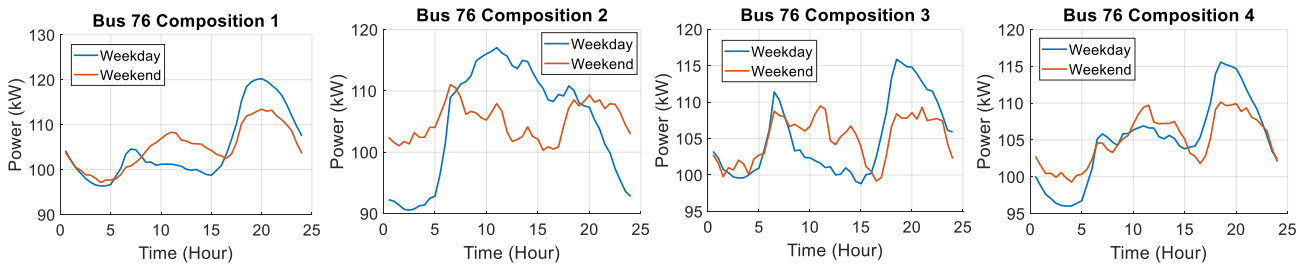

Fig. 7: Aggregated load profiles at POI of bus 76 phase A with four compositions

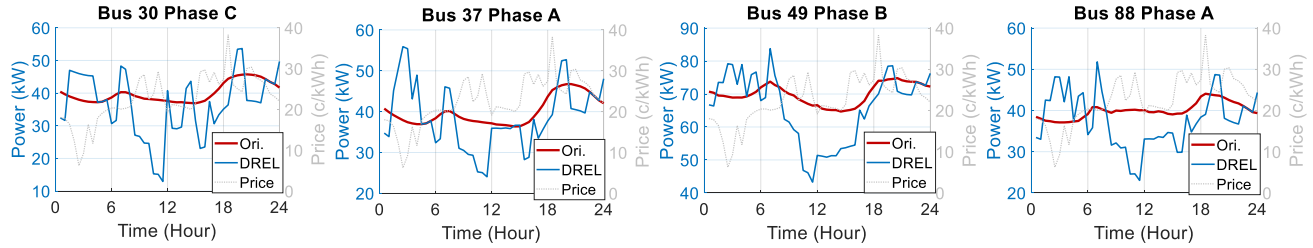

Fig. 8: Samples of DREL and conventional load profiles

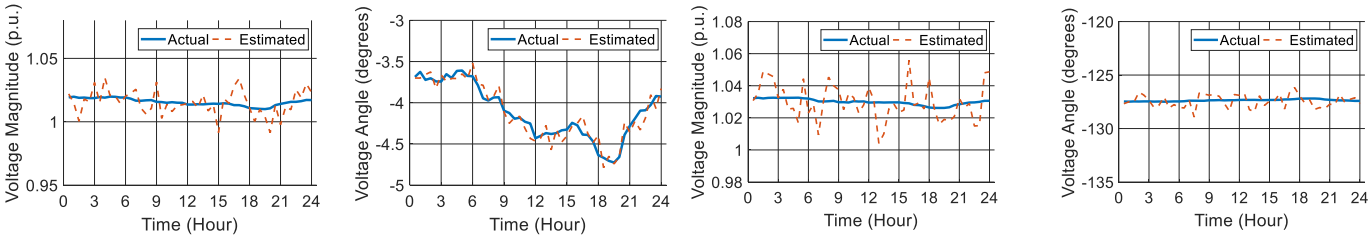

(a) Voltage magnitude and angle at Bus 8.1

(b) Voltage magnitude and angle at Bus 54.2

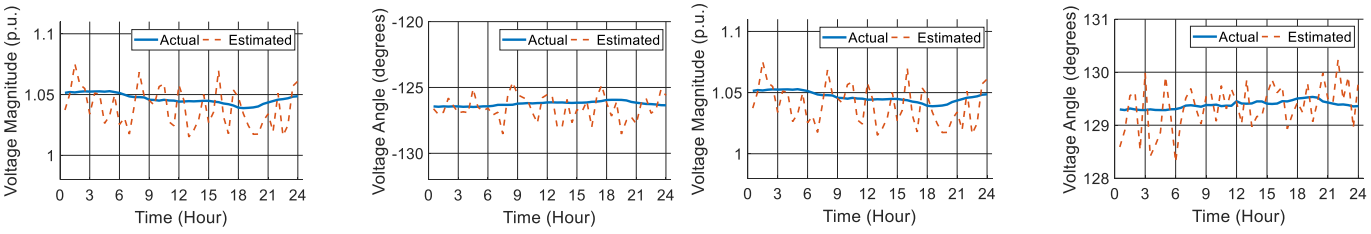

(c) Voltage magnitude and angle at Bus 93.2

(d) Voltage magnitude and angle at Bus 26.3

Fig. 9: Actual and estimated results for voltage magnitude and angles at Bus 8.1, 54.2, 93.2, and 26.3

can better capture the DREL responsiveness to a special energy price. While the existing method has a dataset of historical data; when the energy price is uncommon, it may generate a less accurate pseudo-measurements.

D. Sensitivity Study

At last, we study the impacts of the DREL penetration level and parameter estimation accuracy on the estimation accuracy.

Recall that in the previous case studies, we assume the DREL penetration level to be approximately 15%. In this subsection, we further consider the following scenarios: 5, 20, 30, 50 buses are penetrated by DRELs, aside from the original 10-bus case. They correspond to 5.7%, 26.4%, 37.9% and 45.8% of the total demand, respectively. For each scenario, we conduct two sets of simulations (1000 simulations each set): one is conducted when the proposed work is applied; and the other is conducted using the new benchmark method where DREL historical data are used to generate pseudo-measurements. The RMSEs are computed, which are shown in Table III. It can be observed that with the increase of DREL penetration levels, the estimation errors of our approach and the benchmark both increase in general. This shows that the penetration level of DRELs can influence the estimation accuracy. One reason is that we consider a variety of uncertain components in a DREL, which amounts to the variability of their output profiles. It could be more difficult for a state estimator to capture the increased variability. Consequently, the estimation accuracy is influenced. However, our approach

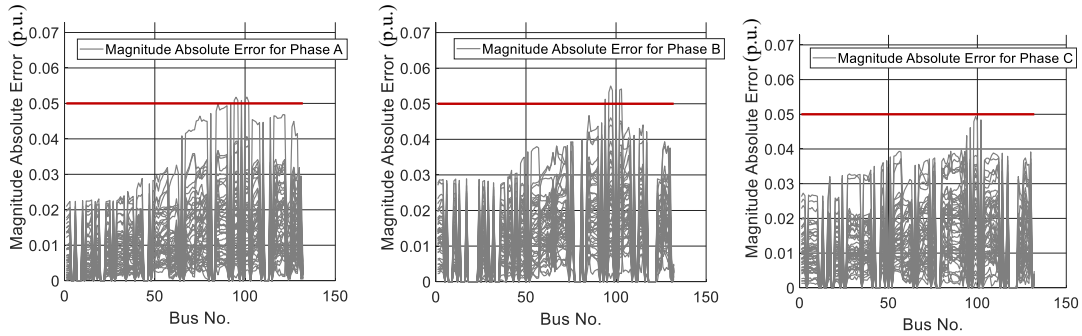

Fig. 10: Absolute errors for voltage magnitude

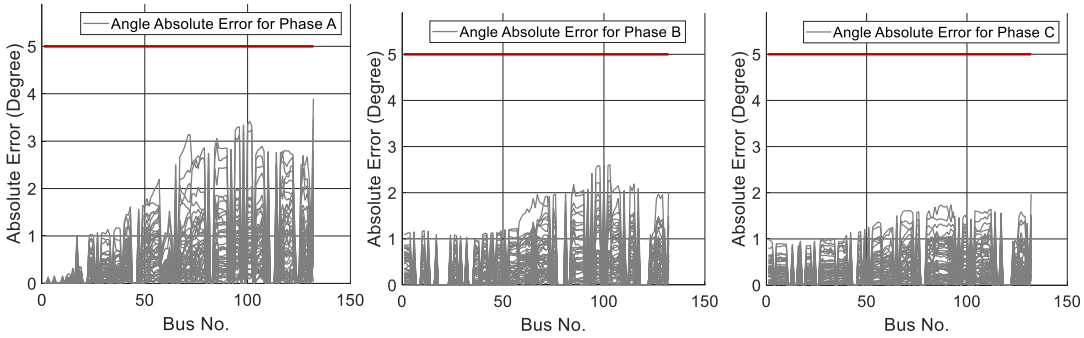

Fig. 11: Absolute errors for voltage phase angles

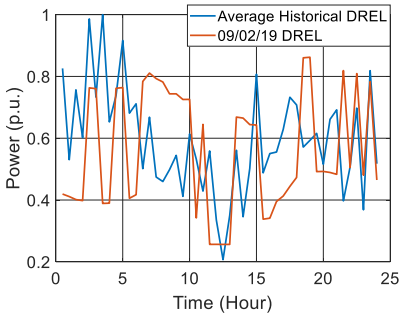

Fig. 12: Comparison between expected and actual DREL consumption profiles

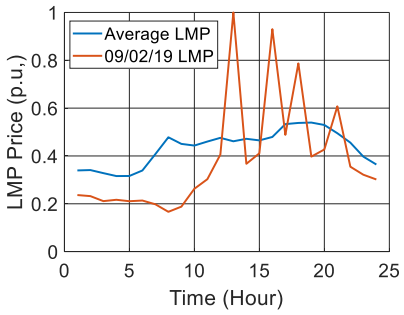

Fig. 13: Comparison between average and actual LMP energy price

outperforms the benchmark in all the considered penetration levels. One reason is that our approach tackles specifically of the variability with respect to the current energy prices, instead of solely relying on the historical data to estimate such variability. This further shows the advantage of the proposed work.

TABLE III: Estimation Accuracy with Different DREL Penetration Levels

No. DREL Buses	Prop. Appr. RMSE (%)	Benchmark RMSE (%)
5	1.01	1.11
10	2.08	5.78
20	2.19	5.81
30	2.27	6.21
50	2.48	6.92

In addition, we conduct sensitivity study with respect to the parameters in the DREL model. In previous case studies the bounds of the SOC are assumed to be known and are set as $[0.1, 0.9]$. In the sensitivity study, we still assume the SOC bounds in the DREL model to be $[0.1, 0.9]$; meanwhile, the actual SOC bounds are $[0.1, 0.9]$, $[0.05, 0.95]$, $[0.15, 0.85]$, $[0.2, 0.8]$, $[0.3, 0.7]$, and $[0.45, 0.55]$, respectively. For each scenario, we conduct 1000 simulation trials to obtain the averaged RMSEs. The results are summarized in Table IV. Notice that the first row is the scenario where the actual SOC bounds match those used in the model. It can be seen that when the difference in the estimated and actual SOC bounds are relatively small (e.g, when the estimated error is less than ± 0.2), the estimation accuracy is reasonable. However, when the difference is too large, the estimation

result is highly inaccurate, as in the case with the actual SOC range $[0.45, 0.55]$. It should be pointed out that we have four to eight ESSs for each DREL penetrated nodes; and each ESS has a capacity of 20 kWh. In the IEEE 123-bus system that we use for the testing many buses have a real power injection of 40 kW or less, hence the perturbations of ± 0.2 to the estimated SOC bounds are non-trivial and they show the reasonable estimation accuracy of the proposed work. Another insight from the results is that though our approach can still have reasonably good estimation results with moderate DREL modeling errors, the estimation accuracy can be improved if more accurate DREL model is available. Potential methods to improve the model fidelity includes: 1) DRELs can be incentivized to provide some operating parameters like SOC operating range to the utility; 2) utility can employ advanced load disaggregation methods to find the required information [33].

TABLE IV: Sensitivity to Perturbations of SOC Bounds

Actual SOC Bounds	RMSE (%)
$[0.1, 0.9]$	2.08
$[0.05, 0.95]$	2.11
$[0.15, 0.85]$	2.25
$[0.2, 0.8]$	2.74
$[0.3, 0.7]$	5.76
$[0.45, 0.55]$	33.6

V. Conclusion

This paper reports improved performance of a state estimator for a distribution system with new characterization of significant DRELs in the system. A DREL has more diverse power consumption characteristics than a conventional load in that it has strong responsiveness to a time-varying price signal. Historic conventional load profiles cannot characterize this responsiveness, and it poses challenges for generating pseudo-measurement for DSSE. We develop a new online pseudo-measurement characterization to tackle this issue. We formulate an optimization model to emulate a DREL's self-interested decision making mechanism. The uncertainty and different compositions of a DREL are modeled as unknown parameters of the model. We use a sampling-based method from stochastic optimization techniques to solve the optimization problem. The optimization results constitute a set of representative DREL profiles amenable to pseudo-measurement generation. The proposed approach is generic and can be easily extended to pseudo-measurement characterization of loads responsive to any other signal related to grid services, like voltage support, frequency support, spinning reserve, among others. Simulation case studies based on IEEE 123-bus test systems as well as real-world data verify the validity of the proposed work.

Appendix A
Details of Model

Compact state and control representations of the individual components are given as follows:

$$\text{Aggregate ESS state:} \quad x_i^{\mathrm{B}} = \left[SOC_{i,1}, \cdots, SOC_{i,n^{\mathrm{B}}}\right]^\top$$

$$\text{Aggregate HVAC state:} \quad x_i^{\mathrm{H}} = \left[T^{\mathrm{I}}_{i,1}, \cdots, T^{\mathrm{I}}_{i,n^{\mathrm{H}}}\right]^\top$$

$$\text{Aggregate PEV state:} \quad x_i^{\mathrm{V}} = \left[RC_{i,1}, \cdots, RW_{i,n^{\mathrm{V}}}\right]^\top$$

$$\text{Aggregate ESS control:} \quad u_i^{\mathrm{B}} = \left[u^{\mathrm{Bc}}_{i,1}, \cdots, u^{\mathrm{Bd}}_{i,n^{\mathrm{B}}}\right]^\top$$

$$\text{Aggregate HVAC control:} \quad u_i^{\mathrm{H}} = \left[u^{\mathrm{H}}_{i,1}, \cdots, u^{\mathrm{H}}_{i,n^{\mathrm{H}}}\right]^\top$$

$$\text{Aggregate PEV control:} \quad u_i^{\mathrm{V}} = \left[u^{\mathrm{RC}}_{i,1}, \cdots, u^{\mathrm{RW}}_{i,n^{\mathrm{V}}}\right]^\top$$

The aggregate state, control, output, and uncontrollable disturbance variables of node i are given by

$$\text{Aggregate node } i \text{ state:} \quad x_i = [(x_i^{\mathrm{B}})^\top, (x_i^{\mathrm{H}})^\top, (x_i^{\mathrm{V}})^\top]^\top$$

$$\text{Aggregate node } i \text{ control:} \quad u_i = [(u_i^{\mathrm{B}})^\top, (u_i^{\mathrm{H}})^\top, (u_i^{\mathrm{V}})^\top]^\top$$

$$\text{Aggregate node } i \text{ disturbance:} \quad w_i = [T_i^{\mathrm{A}}, E_i^{\mathrm{L}}, E_i^{\mathrm{PV}}]^\top$$

System and control matrices can be easily obtained from the individual models as well. For example, if the system has one of each DREL component, these matrices are as follows:

$$A_i = \begin{bmatrix} 1 & & & \\ & a & & \\ & & 1 & \\ & & & 1 \end{bmatrix} \quad G = \begin{bmatrix} \Delta S\bar{O}C_i & & & \\ & (1-a)R\Delta\bar{E}_i^{\mathrm{H}} & & \\ & & 1 & \\ & & & 1 \end{bmatrix}$$

$$B_{2i} = G \cdot \begin{bmatrix} \eta_i^{\mathrm{c}} & -1/\eta_i^{\mathrm{d}} & & & \\ & & 1 & -1 & \\ & & & -1 & \\ & & & & -1 \end{bmatrix}$$

$$B_{1i} = \begin{bmatrix} 0 & 0 & 0 \\ 1-a & 0 & 0 \\ 0 & 0 & 0 \\ 0 & 0 & 0 \end{bmatrix} \quad D_{2i}^\top = [\bar{E}_i^{\mathrm{B}}, -\bar{E}_i^{\mathrm{B}}, (1-a)\Delta E_i^{\mathrm{H}}, (1-a)\Delta E_i^{\mathrm{H}}, \bar{E}_i^{\mathrm{V}}, 0]^\top$$

$$D_{1i}^\top = [0,\ 1,\ 1]^\top.$$

References

[1] E. Manitsas, R. Singh, B. C. Pal, and G. Strbac, "Distribution system state estimation using an artificial neural network approach for pseudo measurement modeling," *IEEE Trans. Power Syst.*, vol. 27, no. 4, pp. 1888–1896, Nov 2012.

[2] A. Primadianto and C.-N. Lu, "A review on distribution system state estimation," *IEEE Trans. Power Syst.*, vol. 32, no. 5, pp. 3875–3883, 2016.

[3] F. C. Schweppe and J. Wildes, "Power system static-state estimation, part i: Exact model," *IEEE Transactions on Power Apparatus and Systems*, vol. PAS-89, no. 1, pp. 120–125, Jan 1970.

[4] M. E. Baran and A. W. Kelley, "A branch-current-based state estimation method for distribution systems," *IEEE transactions on power systems*, vol. 10, no. 1, pp. 483–491, 1995.

[5] L. Mili, M. G. Cheniae, N. S. Vichare, and P. J. Rousseeuw, "Robust state estimation based on projection statistics [of power systems]," *IEEE Trans. Power Syst.*, vol. 11, no. 2, pp. 1118–1127, May 1996.

[6] A. Monticelli, "Electric power system state estimation," *Proceedings of the IEEE*, vol. 88, no. 2, pp. 262–282, 2000.

[7] A. Abur and A. G. Exposito, *Power system state estimation: theory and implementation*. CRC press, 2004.

[8] G. B. Giannakis *et al.*, "Monitoring and optimization for power grids: A signal processing perspective," *IEEE Signal Processing Magazine*, vol. 30, no. 5, pp. 107–128, 2013.

[9] J. Zhao *et al.*, "Power system real-time monitoring by using pmu-based robust state estimation method," *IEEE Transactions on Smart Grid*, vol. 7, no. 1, pp. 300–309, Jan 2016.

[10] J. Zhao, M. Netto, and L. Mili, "A robust iterated extended kalman filter for power system dynamic state estimation," *IEEE Transactions on Power Systems*, vol. 32, no. 4, pp. 3205–3216, July 2017.

[11] K. Dehghanpour *et al.*, "A survey on state estimation techniques and challenges in smart distribution systems," *IEEE Trans. Smart Grid*, vol. 10, no. 2, pp. 2312–2322, 2018.

[12] G. Wang, G. B. Giannakis, J. Chen, and J. Sun, "Distribution system state estimation: An overview of recent developments," *Frontiers of Information Technology & Electronic Engineering*, vol. 20, no. 1, pp. 4–17, 2019.

[13] W. W. Kotiuga and M. Vidyasagar, "Bad data rejection properties of weughted least absolute value techniques applied to static state estimation," *IEEE Transactions on Power Apparatus and Systems*, no. 4, pp. 844–853, 1982.

[14] L. M. V. Phaniraj, "Least median of squares estimation in power systems," *IEEE Transactions on Powcr Sysucms*, vol. 6, no. 2, 1991.

[15] A. Primadianto and C. Lu, "A review on distribution system state estimation," *IEEE Transactions on Power Systems*, vol. 32, no. 5, pp. 3875–3883, 2017.

[16] A. K. Ghosh, D. L. Lubkeman, M. J. Downey, and R. H. Jones, "Distribution circuit state estimation using a probabilistic approach," *IEEE Trans. Power Syst.*, vol. 12, no. 1, pp. 45–51, 1997.

[17] S. Bhela, V. Kekatos, and S. Veeramachaneni, "Enhancing observability in distribution grids using smart meter data," *IEEE Transactions on Smart Grid*, vol. 9, no. 6, pp. 5953–5961, 2018.

[18] R. Singh, B. Pal, and R. Jabr, "Distribution system state estimation through gaussian mixture model of the load as pseudo-measurement," *IET generation, transmission & distribution*, vol. 4, no. 1, pp. 50–59, 2010.

[19] A. Angioni, T. Schlösser, F. Ponci, and A. Monti, "Impact of pseudo-measurements from new power profiles on state estimation in low-voltage grids," *IEEE Transactions on Instrumentation and Measurement*, vol. 65, no. 1, pp. 70–77, 2016.

[20] K. Dehghanpour, Y. Yuan, Z. Wang, and F. Bu, "A game-theoretic data-driven approach for pseudo-measurement generation in distribution system state estimation," *IEEE Transactions on Smart Grid*, vol. 10, no. 6, pp. 5942–5951, 2019.

[21] M. E. Baran, J. Zhu, and A. W. Kelley, "Meter placement for real-time monitoring of distribution feeders," *IEEE Transactions on Power systems*, vol. 11, no. 1, pp. 332–337, 1996.

[22] A. Shafiu, N. Jenkins, and G. Strbac, "Measurement location for state estimation of distribution networks with generation," *IEE Proceedings-Generation, Transmission and Distribution*, vol. 152, no. 2, pp. 240–246, 2005.

[23] F. F. Wu, "Power system state estimation: a survey," *International Journal of Electrical Power & Energy Systems*, vol. 12, no. 2, pp. 80–87, 1990.

[24] Ke Li, "State estimation for power distribution system and measurement impacts," *IEEE Trans. Power Syst.*, vol. 11, no. 2, pp. 911–916, May 1996.

[25] R. Singh, B. C. Pal, and R. A. Jabr, "Statistical representation of distribution system loads using gaussian mixture model," *IEEE Transactions on Power Systems*, vol. 25, no. 1, pp. 29–37, 2009.

[26] G. Irwin, W. Monteith, and W. Beattie, "Statistical electricity demand modelling from consumer billing data," in *IEE Proceedings C (Generation, Transmission and Distribution)*, vol. 133, no. 6. IET, 1986, pp. 328–335.

[27] D. Gerbec, S. Gasperic, I. Smon, and F. Gubina, "Allocation of the load profiles to consumers using probabilistic neural networks," *IEEE Transactions on Power Systems*, vol. 20, no. 2, pp. 548–555, 2005.

[28] J. Wu, Y. He, and N. Jenkins, "A robust state estimator for medium voltage distribution networks," *IEEE Trans. Power Syst.*, vol. 28, no. 2, pp. 1008–1016, 2012.

[29] B. P. Hayes, J. K. Gruber, and M. Prodanovic, "A closed-loop state estimation tool for mv network monitoring and operation," *IEEE Trans. Smart Grid*, vol. 6, no. 4, pp. 2116–2125, 2014.

[30] O. Erdinc, N. G. Paterakis, T. D. Mendes, A. G. Bakirtzis, and J. P. Catalao, "Smart household operation considering bi-directional ev and ess utilization by real-time pricing-based dr," *IEEE Transactions on Smart Grid*, vol. 6, no. 3, pp. 1281–1291, 2014.

[31] R. E. Mortensen and K. P. Haggerty, "A stochastic computer model for heating and cooling loads," *IEEE Transactions on Power Systems*, vol. 3, no. 3, pp. 1213–1219, 1988.

[32] S. Ahmadi, S. Bathaee, and A. H. Hosseinpour, "Improving fuel economy and performance of a fuel-cell hybrid electric vehicle (fuel-cell, battery, and ultra-capacitor) using optimized energy management strategy," *Energy Conversion and Management*, vol. 160, pp. 74–84, 2018.

[33] H. Ahmadi and J. R. Martı, "Load decomposition at smart meters level using eigenloads approach," *IEEE transactions on Power Systems*, vol. 30, no. 6, pp. 3425–3436, 2015.

[34] A. Sankarakrishnan and R. Billinton, "Sequential monte carlo simulation for composite power system reliability analysis with time varying loads," *IEEE Transactions on Power Systems*, vol. 10, no. 3, pp. 1540–1545, 1995.

[35] C. Singh, P. Jirutitijaroen, and J. Mitra, *Monte Carlo Simulation*, 2019, pp. 165–183.

[36] O. Dzobo, K. Alvehag, C. Gaunt, and R. Herman, "Multi-dimensional customer segmentation model for power system reliability-worth analysis," *International Journal of Electrical Power & Energy Systems*, vol. 62, pp. 532–539, 2014.

[37] M. Grant and S. Boyd, "CVX: Matlab software for disciplined convex programming, version 2.1," http://cvxr.com/cvx, Mar. 2014.

[38] IEEE 123 bus Feeder. [Online]. Available: https://site.ieee.org/pes-testfeeders

[39] Haibin Wang and N. N. Schulz, "A revised branch current-based distribution system state estimation algorithm and meter placement impact," *IEEE Transactions on Power Systems*, vol. 19, no. 1, pp. 207–213, 2004.

[40] C. C. S. LLC, "CT accuracy standards." [Online]. Available: https://ctlsys.com/support/ct-accuracy-standards/

[41] ——, "AN-136 metering system accuracy." [Online]. Available: https://ctlsys.com/wp-content/uploads/2017/04/AN-136-Metering-System-Accuracy-AppNote.pdf

[42] NREL Solar Radiation Research Laboratory. [Online]. Available: https://midcdmz.nrel.gov/apps/sitehome.pl?site=BMS

[43] PJM, "PJM energy & ancillary services market operations." [Online]. Available: https://pjm.com/~/media/documents/manuals/m11.ashx

[44] ——, "Pjm locational marginal pricing (lpm) data." [Online]. Available: https://dataminer2.pjm.com/feed/rt_da_monthly_lmps/definition

Jianzhe Liu (S'13-M'18) received the B.E. degree in electrical engineering from Huazhong University of Science and Technology, China, in 2012, and the Ph.D. degree in electrical and computer engineering from The Ohio State University, US, in 2017. Dr. Liu was a visiting scholar at Aalborg University, Denmark, in 2017. He is currently an Energy Systems Scientist at Argonne National Laboratory. His research interests include robust control and optimization for electric power systems. He is a recipient of the Argonne Outstanding Postdoc Award.

Ravindra Singh (M'09-SM'20) is a Principal Distribution Engineer at Argonne National Laboratory. He received the B.Tech. (with honors) degree from HBTI, Kanpur, India, the M.Sc. Engg.) degree from the Indian Institute of Science, Bangalore, India, and the Ph.D. degree from Imperial College London, London, U.K., in 2002, 2004, and 2009, respectively, all in electrical engineering.

Prior to joining Argonne he has worked with ABB Corporate Research Center and Honeywell. His current research focus is in the area of power system operation and control with particular emphasis on renewable integration, distribution system state estimation, distribution automation and cyber-security of power systems. Dr. Singh is also active in professional activities. He is a chair of IEEE working group on distribution system state estimation and also serves as an editor of IEEE transactions on sustainable energy.

Bikash C. Pal (M'00-SM'02-F'13) received B.E.E. (with honors) degree from Jadavpur University, Calcutta, India, M.E. degree from the Indian Institute of Science, Bangalore, India, and Ph.D. degree from Imperial College London, London, U.K., in 1990, 1992, and 1999, respectively, all in electrical engineering. Currently, he is a Professor in the Department of Electrical and Electronic Engineering, Imperial College London.

His current research interests include renewable energy modelling and control, state estimation, and power system dynamics. He is Vice President Publications, IEEE Power & Energy Society. He was Editor-in-Chief of IEEE Transactions on Sustainable Energy (2012-2017) and Editor-in-Chief of IET Generation , Transmission and Distribution (2005-2012) and is a Fellow of IEEE for his contribution to power system stability and control.